FACHBEITRAG

Numerical simulation of spatial temperature and salinity distribution in the Waiwera geothermal reservoir, New Zealand

Thomas Kempka[1,2] (iD) · Michael Kühn[1,2]

Abstract

The geothermal reservoir in Waiwera was not sustainably managed for many decades. Hence, the responsible authority introduced a water management concept, whereby various independent models were developed and calibrated using observations. As these models were not yet able to reproduce all observations, constant model revisions are critical for efficient reservoir management. Results of a recent field campaign were used for the current model revision, considering two new main structural geological findings to reconstruct the natural reservoir state. Our simulation results demonstrate that a recently proven north-south trending fault in the study area plays a key role in improving the model. Further analysis suggests the presence of a not yet confirmed additional west-east aligned geologic fault in the north, since thermal convection is observed inland. Additional field campaigns are needed to acquire more information on the main geological fault zones as well as additional data on temperature and salinity distributions.

Keywords Numerical simulation · Geothermal reservoir · Geologic faults · Temperature · Freshwater-saltwater interface

Numerische Simulation der räumlichen Temperatur- und Salinitätsverteilung im geothermischen Reservoir Waiwera, Neuseeland

Zusammenfassung

Das geothermische Reservoir in Waiwera wurde über Jahrzehnte nicht nachhaltig bewirtschaftet. Folglich hat die zuständige Behörde ein Wassermanagementkonzept eingeführt, in dessen Rahmen eine Vielzahl unabhängiger Modelle entwickelt und mithilfe von Beobachtungen kalibriert wurde. Eine ständige Überarbeitung der bestehenden Simulationsmodelle ist hierbei erforderlich, da noch keines alle Beobachtungen zuverlässig reproduzieren kann. In der vorliegenden Studie wurden Ergebnisse einer aktuellen Feldkampagne für die Überarbeitung eines bestehenden Modells verwendet. Insbesondere wurden dazu zwei neue geologische Strukturen berücksichtigt, um den natürlichen Zustand des Reservoirs zu rekonstruieren. Die Simulationsergebnisse zeigen, dass eine neu belegte Nord-Süd-Störungszone im Untersuchungsgebiet eine wesentliche Rolle für die Präzisierung der Modelle spielt. Weiterhin unterstreicht die Ergebnisanalyse, dass eine zusätzliche, bisher nicht nachgewiesene West-Ost-Störungszone im Norden des Untersuchungsgebiets vorhanden sein muss, da eine landeinwärts auftretende thermische Konvektion nur mithilfe dieser erklärt werden kann. Weitere Feldkampagnen sind notwendig, um zusätzliche Informationen zu den geologischen Hauptstörungszonen sowie Daten zur Temperatur- und Salinitätsverteilung zu gewinnen.

Schlüsselwörter Numerische Simulation · Geothermisches Reservoir · Geologische Störungszonen · Temperatur · Versalzung

✉ Thomas Kempka
  thomas.kempka@gfz-potsdam.de

  Michael Kühn
  michael.kuehn@gfz-potsdam.de

[1] GFZ German Research Centre for Geosciences, Telegrafenberg, 14473 Potsdam, Germany

[2] Institute of Geosciences, University of Potsdam, Karl-Liebknecht-Str. 24–25, 14476 Potsdam, Germany

Introduction

The geothermal reservoir in Waiwera has been known for a long time and has been used for balneological purposes since the 19th century, but it was not sustainably managed for many decades, so that, among other things, the natural artesian flow from the wells ceased and hot water springs on the beach dried up. This circumstance prompted the Auckland Council as responsible authority to introduce a water management plan. For this purpose and to help better understand the system, various geological models (Alldred 1980; Alvarez 1986) as well as analytical (Chapman 1998; Kühn and Grabow 2021; Kühn and Schöne 2017) and numerical simulation models (Alvarez 1986; Bréthaut 2009; Kühn and Stöfen 2005; Somogyvári et al. 2019) have been developed since the 1980s, but so far they do not represent the essential observations and processes in the reservoir with sufficient accuracy. For this reason, the continuous improvement of existing hydrogeological models of the Waiwera reservoir based on new observations and findings from field campaigns represents an essential contribution to management planning. The aim is to ensure the sustainable use of the natural resource in order to preserve this historic and tourist site (Auckland Regional Water Board 1980, 1987).

Within the framework of any sustainable water management, it is necessary to build up a system understanding, and subsequently a hydrogeological model that is capable of describing the actual hydraulic and thermal conditions. As mentioned before, models of varying complexity have been created since the 1980s, and which have been compared with each other (Kühn et al. 2016). Overall, it can be said that the various model approaches provide answers to partial aspects that improve the resource management of the geothermal reservoir. However, there is still no mathematical model that can be used for a quantified management (i.e. forecasting) that integrates all available observation data and is based on the exact geometry and location of the boreholes and temperature and salinity distributions for different exploitation scenarios (Kühn et al. 2016). To create such a model, further field investigations were recommended (Zermansky 2005).

The results of a photogrammetric outcrop mapping conducted at Waiwera Beach in 2019 (Präg et al. 2020) were used in the present study to further improve an established 3D hydrogeological model of the geothermal reservoir (Kühn and Stöfen 2005) using coupled numerical flow and transport simulations (Kempka 2020). In particular, newly gained structural geological and lithological knowledge was taken into account to calibrate the model based on borehole data and to reconstruct the natural state of the geothermal reservoir.

Materials and methods

The following subsections introduce the hydrogeological setting of the study area, the preliminary modelling work related to the Waiwera geothermal reservoir as well as the numerical model and investigated hydrogeological hypotheses.

Hydrogeological setting

Waiwera is a small coastal village located on New Zealand's North Island, about 40 km north of Auckland. It is located on the southern bank of the Waiwera River, between the Wenderholm Regional Park in the north and the Waiwera Hill Scenic Reserve in the south. Waiwera was known by the Maori people for its natural hot springs, which originated from the geothermal aquifer below the village (Auckland Regional Water Board 1980).

The Waiwera reservoir is located within the Pakiri Formation (Fig. 1) of the Early Miocene Waitemata Group (Schofield 1989). The geothermal reservoir below Waiwera consists of compacted and cemented sandstones and siltstones of the Waitemata Group. These are up to 425 m thick and were folded, faulted and fractured by tectonic movement throughout their entire depth. Unconsolidated alluvial and marine sands, silts and clays with a thickness of some 10 m that form the sandspit on which Waiwera was build, act as a seal for the underlying reservoir (Auckland Regional Water Board 1980). Near Waiwera, beds and formations are seen to dip 20–25° north-west.

The reservoir rocks are outcropping in the hills surrounding the township and in the cliffs at either side of Waiwera beach (Auckland Regional Water Board 1980). The outcrop standing south of Waiwera beach is a good example (Präg et al. 2020). The folds and faults are observed mainly to trend east-west (Präg 2020). The east-west Waiwera Fault is assumed to be a deep structure possibly affecting the reservoir as well. It is described by Alldred (1980) based on field observations at Mahurangi Island as well as on the elevation of the top of the greywacke from borehole logs (Auckland Regional Water Board 1980).

Most importantly, the findings of Präg (2020) have confirmed that a major structural feature in approximately a north-south direction exists, which was always presumed from the Auckland Regional Water Board (1980) but so far not detected due to missing obvious features at the surface. This is a system-relevant feature that is part of the existing 3D geological models (Kühn and Stöfen 2005; Kühn et al. 2022) and is investigated further in the present study.

The thermal water has a temperature of approximately 50 °C at 150 m depth and is believed to be of meteoric origin due to its chemical composition and the enclosed gases (mainly nitrogen and carbon dioxide are only present in
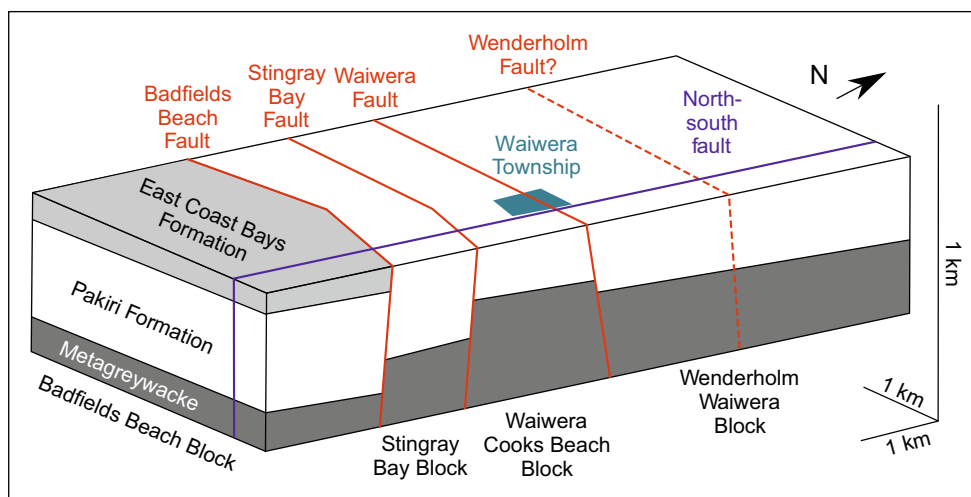
Fig. 1 Schematic of tectonic block structure and geologic faults in the vicinity of the study area (adapted from Alldred 1980, and Bréthaut 2009). The presence of the north-south fault has been recently proven by the geologic mapping undertaken by Präg (2020). An additional fault trending in east-west direction (Wenderholm Fault) is suggested by temperature observations

Abb. 1 Schematische Übersicht der tektonischen Blockstruktur und Störungszonen im Umfeld des Untersuchungsgebiets (verändert nach Alldred 1980 und Bréthaut 2009). Die in Nord-Süd-Richtung streichende Störungszone wurde kürzlich durch eine geologische Kartierung bestätigt (Präg 2020). Beobachtungsdaten der Temperatur belegen darüber hinaus die Präsenz einer weiteren in West-Ost-Richtung streichenden Störungszone (Wenderholm-Störungszone)

traces, no hydrogen sulphide was found), which preclude a volcanic origin. It is further assumed that the thermal water is sourced by rain water from further inland, which percolates to a depth between 1200 and 2200 m (indicated by the silica content of the thermal water) and moves seawards, while being heated by a temperature gradient of about 30 °C per kilometre (Auckland Regional Water Board 1980).

The recent conceptual model assumes that the thermal water enters the aquifer by rapidly rising through a junction of the newly proven north trending feature and the major east-west oriented Waiwera Fault within the greywacke basement rock. However, the existence of this fault zone has not been proven, since there is no direct evidence for its existence at the surface (Auckland Regional Water Board 1980). A pump test, which was carried out in April 1979, indicated a fairly homogeneous composition of the aquifer with a calculated transmissivity of 320 m² per day which represents a hydraulic conductivity of approximately $2.3 \cdot 10^{-5}$ m s^{-1} (Kühn and Stöfen 2005). Due to the comparably high transmissivity for a Waitemata Group aquifer, it is assumed that the pathways for groundwater flow within the aquifer are provided by fractures rather than pores, which further form the leakage paths to the hot springs (Zermansky 2005).

In addition to the geothermal water recharging the aquifer from below, there are two more types of water entering the aquifer. An influx of cold, fresh, near-surface groundwater is topographically-driven into the aquifer from the west, while seawater is believed to intrude through the hot spring leakage paths on the foreshore in the east

like elsewhere along the coast (Auckland Regional Water Board 1980; Kühn and Stöfen 2005). The intruding cold groundwater and seawater have the potential to irreversibly alter the hydraulic conditions of the geothermal reservoir, if the convective upwelling of thermal water is suppressed. Therefore, the abstraction rates from the reservoir have been monitored since 1986, following the water allocation and management plan.

Preliminary modelling work

A reservoir model of the Waiwera geothermal system was developed by Alvarez (1986). Data were compiled for the programme SHAFT 79 (Pruess and Schroeder 1979) to create a two-dimensional model of the study area which was used to address questions of geothermal production. The results suggested that the inflow of geothermal water from below into the reservoir should be in the order of 20 kg s^{-1}, corresponding to an energy recovery of 4 MW. The associated scenario analysis showed that this allows for a permanent production rate of about 1750 m³ per day.

Chapman (1998) investigated the dynamics of the Waiwera geothermal system and attempted to develop a predictive model of the Waiwera system by applying a standard Theis modelling approach to identify the relevant variables between water levels in the monitoring borehole and water extraction by the five largest users. From the best fit of his analytical model, he concluded that there is a strong pumping signal in the water level record of the monitoring borehole. He estimated that the Auckland Council manage-

ment objective could be achieved with a constant pumping rate of 970 m³/day. This approach produced very good results but was tied to specific wells which are no longer in service.

Previous work on the geothermal reservoir in Waiwera includes a reactive flow model of the reservoir Waiwera by Kühn and Stöfen (2005), which presents a numerical simulation including fluid flow, heat transfer and chemical reactions and was used to test the proposed conceptual model of the geothermal field. In this model, the mentioned north-south trending fault is a significant structural feature through which an inflow rate of the geothermal water was implemented as determined by Alvarez (1986). It visualises the distribution of geothermal water, freshwater and seawater within the aquifer, along with the chloride concentration and calcite equilibrium. This model has been used in the presented study and is further referred to as a reference model.

Bréthaut (2009) applied the TOUGH2 code (Pruess et al. 1999) to model the Waiwera geothermal system and showed that the conditions within the Waiwera geothermal reservoir needed a numerical model that allows simulating the coupled processes of groundwater flow, heat and solute mass transport. In contrast to Kühn and Stöfen (2005), a focus of that study was a new and deeper model, as well accounting for the topography to assess if large-scale convection through the faults could be the origin of the local upflow at the site. The results show that—in the case of a homogeneous permeable reservoir—the presence of a hill just north of the township prevents any northward outflow due to a gravity-driven southward groundwater flow. It became clear that the west-east trending fault structures are essential to understand the system.

Kühn and Altmannsberger (2016) discuss the advantages and disadvantages of different models (univariate regression model, multivariate regression model and process-based simulations) and suggested to improve the underlying geological model used for the process simulations to provide a more flexible tool for future and prospective scenarios which cannot be covered by data-driven models.

Since such an improved geological model was not yet available, Kühn and Schöne (2017) set up a new multivariate regression model from water level and production rate time series for the Waiwera geothermal reservoir with the recommendation of annual updates to maintain high-accuracy predictions of water levels, as the exact position of production wells is important to be able to refer to any changes in that regard. This is a disadvantage of all analytical solutions.

The work undertaken by Kühn and Schöne (2018) investigates the suspected influence of earthquakes on the water level inside the reservoir after renewed temporary artesian conditions were recorded directly following the Kaikoura earthquake in 2016. However, a clear correlation between peaks in the water level and the occurrence of earthquakes, other than the Kaikoura earthquake, could not be proven. These are short-term effects which did not seem to have altered the system so far.

Somogyvári et al. (2019) followed a different approach with their reservoir-scale transdimensional fracture network inversion to take into account the complex hydraulic and thermal conditions. Instead of a porous matrix model they used discrete fracture network models (DFNs) to implement the main geological features. This was only a synthetic example to prove the viability of the concept, but indeed the first time such kind of models have been applied to the Waiwera system. The general results indicate that areas exist within the aquifer, where distinct features like fracture or layers of higher conductivity play an important role in regard to the temperature distribution in the reservoir.

Kühn and Grabow (2021) applied a deconvolution well test analysis to a long-term data set of the Waiwera geothermal reservoir based on Von Schroeter et al. (2013). Results deduced from decades of water level data in response to production rates clearly indicate radial flow around and towards the main production well and a leaky flow boundary as a constraint of the system. The former underlines that a continuum approach is valid for the Waiwera reservoir and for the latter it enforces the conceptual assumption of convection due to partly open boundaries. The findings agree very well with prior results of the pumping test from 1979.

Integrating the knowledge gained on the study area's structural geology and hydrogeology from these previous studies, the present work uses new structural geologic findings for a revision of the model calibration to reconstruct the natural state of the geothermal reservoir as documented before its exploitation.

Numerical model implementation

The TRANSPORT Simulation Environment (TRANSPORTSE) was applied as numerical simulator in the present study. TRANSPORTSE uses a finite-difference discretisation to simulate density-driven Darcy flow in porous media, and advective, diffusive and dispersive transport of chemical species as well as conductive and convective transport of heat. All details on the mathematical model implementation and numerical benchmarks are provided in Kempka (2020) and Kempka et al. (2022). The code is implemented using the Python language (Van Rossum and Drake 2009), compiled just-in-time by means of the Python numba library (Lam et al. 2015) resulting in computational times equivalent to low-level language implementations, and parallelised using OpenMP (OpenMP 2008). A flexible coupling to different fluid and rock equa-

Table 1 Numerical model parametrisation applied in the present study, adapted from Kühn and Stöfen (2005) as well as Kühn et al. (2022)
Tab. 1 Parametrisierung der numerischen Modelle in der vorliegenden Studie, verändert nach Kühn und Stöfen (2005) sowie Kühn et al. (2022)

Parameter	Symbol	Unit	Alluvial Deposits	Weathered Sandstone	Waitemata Sandstone
Horizontal Permeability	K_x, K_y	m^2	$2.7 \cdot 10^{-14}$	$2.7 \cdot 10^{-14}$	$5.4 \cdot 10^{-13}$
Vertical Permeability	K_z	m^2	$2.7 \cdot 10^{-14}$	$2.7 \cdot 10^{-14}$	$2.7 \cdot 10^{-13}$
Porosity	φ	–	0.30	0.30	0.12
Rock Compressibility	C_r	Pa^{-1}	$4.5 \cdot 10^{-10}$	$4.5 \cdot 10^{-10}$	$4.5 \cdot 10^{-10}$
Heat Capacity	Cp_r	$kJ\,kg^{-1}\,K^{-1}$	0.75	0.85	0.85
Heat Conductivity	L_r	$W\,m^{-1}\,K^{-1}$	2.5	2.0	2.0
Rock Density	ϱ_r	$kg\,m^{-3}$	2100	2700	2700
Diffusion Coefficient	D_f	$m^2\,s^{-1}$	$5 \cdot 10^{-9}$	$5 \cdot 10^{-9}$	$5 \cdot 10^{-9}$

tions of state (e.g. CoolProp, Bell et al. 2014) as well as geochemical libraries (e.g. PHREEQC, Parkhurst and Appelo 2013) is feasible by its modular implementation (Kempka et al. 2022). TRANSPORTSE has been previously applied to scientific questions related to geothermal reservoirs (Kühn et al. 2022), potash salt dissolution (Steding et al. 2021a, b), seawater intrusion (Chabab et al. 2022), contaminant transport (Otto et al. 2022), permafrost formation and thawing as well as gas hydrate formation (Li et al. 2022a, b).

The reference model used in the present study is fully based on that presented by Kühn and Stöfen (2005), with the parametrisation listed in Table 1. Fluid properties are depending on the concentration of dissolved NaCl, pressure and temperature, and are calculated using the equation of state presented by Driesner and Heinrich (2007). Salinity dependency of viscosity is additionally taken into account by applying the Sharkawy et al. (2010) equation of state,

while specific heat capacities are calculated as function of NaCl concentration and temperature using the findings of Urquhart and Bauer (2015). It is worth to note that viscosity only depends on pressure and temperature in the simulations presented by Kühn and Stöfen (2005). The vertical model discretisation is oriented on the lithology at Waiwera, with the alluvial deposits and weathered sandstones represented by two layers of 13 and 10 m thickness at the model top, followed by the Waitemata sandstone of 390 m thickness discretised by 2 layers à 35 m and 8 layers à 40 m. The reservoir's greywacke base unit is implemented as impermeable boundary at the bottom. The horizontal grid discretisation uses a Tartan-type grid refinement in the vicinity of the Waiwera township with element sizes of 25 m × 25 m increasing to up to 100 m × 100 m at the model boundaries with a total of 81,792 grid elements (Fig. 2).

The general model boundary conditions are the following:

Fig. 2 Simulation grid discretisation in the modelling domain with observation boreholes and implemented lithology. The *white elements* represent the alluvial deposits, *red ones* the weathered sandstone and *blue ones* the Waiwera reservoir consisting of the Waitemata sandstone

Abb. 2 Räumliche Diskretisierung des Modellgitters mit Beobachtungsbohrungen und implementierter Lithologie. *Weiße Elemente* repräsentieren Flussablagerungen, *rote Elemente* stehen für verwitterten Sandstein und *blaue* für den Waitemata-Sandstein (Waiwera-Reservoir)
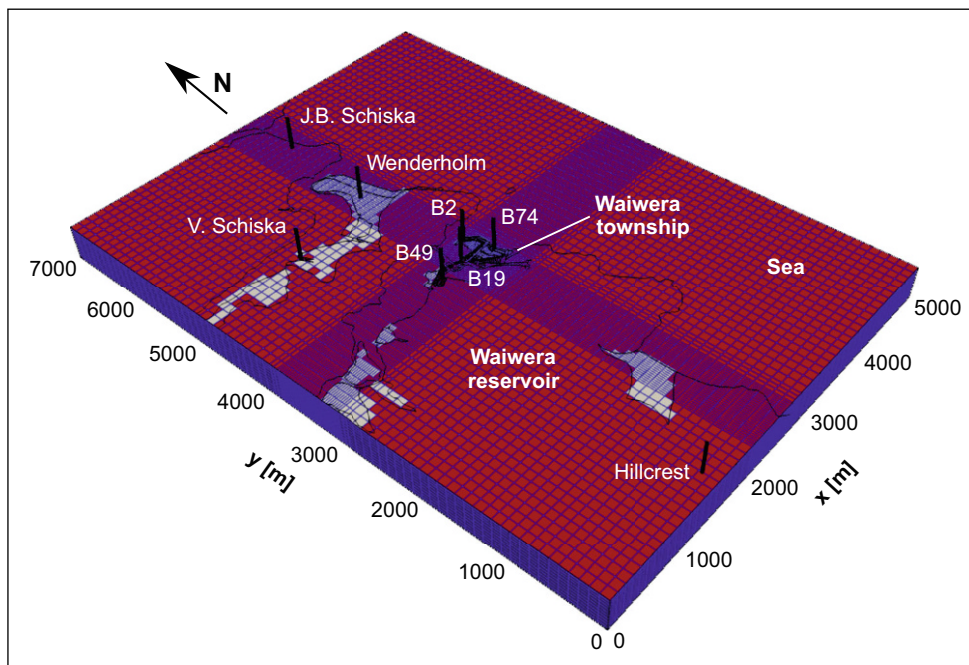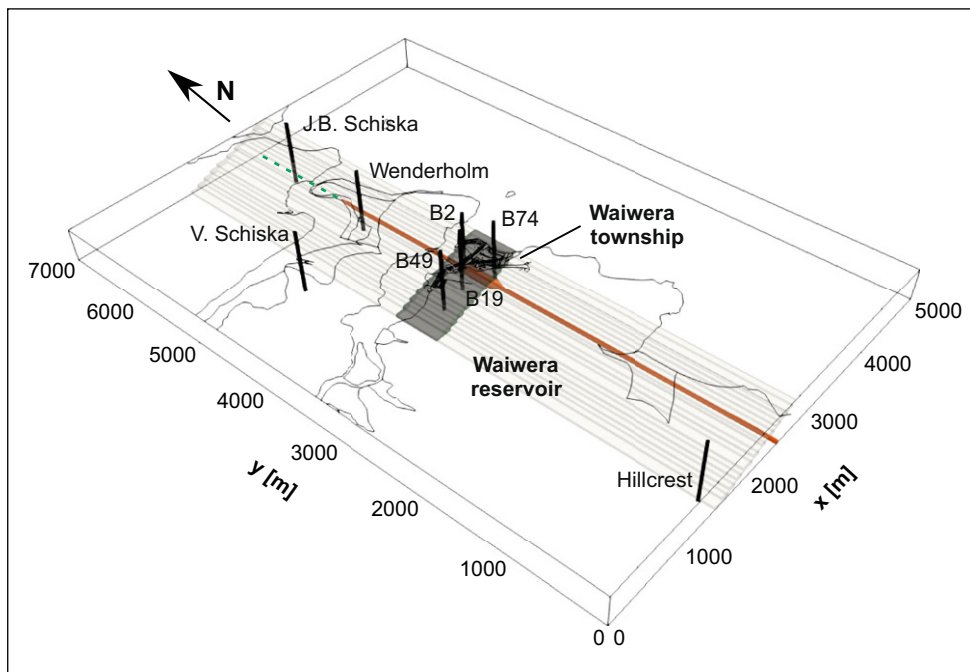
Fig. 3 Location of north-south fault source term in the reference and five hypotheses scenarios in relation to Waiwera township and observation boreholes. Wider areas are parametrised with inflow rates that are higher by one order of magnitude compared to the narrower ones, following the reference model introduced by Kühn and Stöfen (2005). The *green dotted line* indicates the north-south fault section addressed by the changes in the geothermal fluid inflow presented in Hypotheses 1, 2 and 5. The layer of higher permeability dipping into the Waiwera reservoir from the beach front is presented in *transparent light grey colour* (Hypothesis 3), while that limited by block tectonics in its North-South extent is shown in *dark grey colour* (Hypotheses 4 and 5)

Abb. 3 Verortung des Quellterms an der in Nord-Süd-Richtung streichenden Störungszone im Referenzfall und den Simulationen zur Untersuchung der fünf Hypothesen im räumlichen Kontext der Stadt Waiwera und der Beobachtungsbohrungen. Breiter dargestellte Bereiche sind gemäß Kühn und Stöfen (2005) mit einer um eine Größenordnung höheren Zuflussrate im Vergleich zum restlichen Teil der Störungszone parametrisiert. Die *gepunktete grüne Linie* zeigt den Bereich dieser Störungszone, der bezüglich des einströmenden geothermalen Wassers in den Hypothesen 1, 2 und 5 verändert wird. Die höher durchlässige, vom Strand her in das Waiwera-Reservoir einfallende Schicht ist *hellgrau* dargestellt (Hypothese 3), während ihr durch die Blocktektonik begrenzter Bereich *dunkelgrau* illustriert ist (Hypothesen 4 und 5)

- Western boundary: constant sodium chloride (NaCl) concentration at $4\,\mathrm{mmol\,l^{-1}}$, temperatures between 17–28.5 °C determined by the geothermal gradient, implemented by Dirichlet-type boundary conditions, while a Neumann-boundary condition (no-flow or closed boundary) as applied for fluid flow.

- Eastern boundary: constant NaCl concentration at $483\,\mathrm{mmol\,l^{-1}}$ representing seawater, constant pressure as a function of NaCl concentration and depth, and temperatures between 10–21.5 °C determined by the seawater temperature and geothermal gradient and implemented by Dirichlet-type boundary conditions.

- Northern boundary: Neumann-boundary type (no-flow or closed boundary) for fluid flow as well as transport of NaCl and heat.

- Southern boundary: Neumann-boundary type (no-flow or closed boundary) for fluid flow as well as transport of NaCl and heat.

- Bottom boundary: Neumann-boundary type (no-flow or closed boundary) for fluid flow and transport of NaCl and heat. Source term for basal heat flow at $66\,\mathrm{mW\,m^{-2}}$ (Neumann-flow boundary type), source term for geothermal fluid inflow (Neumann-flow boundary type) at the north-south trending fault (see Section Investigated Hypotheses) with a fluid flux of $4.75 \cdot 10^{-7}\,\mathrm{m\,s^{-1}}$ in the north-south fault core elements and one order of magnitude lower in the rest of the fault elements, both resulting in a total inflow of $1750\,\mathrm{m^3 d^{-1}}$ of geothermal fluid. Here, constant temperatures of 50 °C and NaCl concentrations of $32\,\mathrm{mmol\,l^{-1}}$ are applied using a Dirichlet-type boundary condition (Fig. 3).

- Top boundary (see Fig. 2): Sea—constant temperature of 10 °C, NaCl concentration of $483\,\mathrm{mmol\,l^{-1}}$ and hydrostatic pressure based on depth and NaCl concentration; Waiwera reservoir—Neumann-boundary condition type for fluid flow as well as transport of NaCl (no-flow or closed boundary), Dirichlet-type boundary condition for constant temperature with 17 °C; Waiwera township—Neumann-flow boundary condition type with groundwater recharge of $5.87 \cdot 10^{-9}\,\mathrm{m\,s^{-1}}$, constant tem-

perature of 25 °C and NaCl concentration of 4 mmol l⁻¹ (Dirichlet-type boundary condition).

- Initial conditions: pressure following NaCl concentration-dependent fluid density and depth, temperature determined by surface temperature and geothermal gradient, concentration of 4 mmol l⁻¹ for Waiwera reservoir fluid and 483 mmol l⁻¹ for regions below the sea.

Investigated hypotheses

Based on the findings of the photogrammetric mapping of the Waiwera beach region documented by Präg et al. (2020) and the discussion on the recently identified structural geological features in Kühn et al. (2022), five different hypotheses (Table 2) were introduced and simulated, and the results compared against those of the reference model implemented by Kühn and Stöfen (2005) to identify improvements related to the coincidence between observations and simulations. Especially the recently documented north-south trending fault (see Fig. 1) was the focus of the present study in terms of its potential contribution to the entire hydrogeological system.

Further, the dipping layer identified at the Waiwera beach front by Präg et al. (2020) and supported by the findings of Somogyvári et al. (2019), showing increased fluid temperatures, suggest that a hydraulic connection to the Waiwera reservoir exists. Consequently, this hypothesis is also tested by the implementation of a highly permeable dipping layer into the model using two approaches: the first one assumes an extent along the entire north-south dimension of the model, while the second approach considers a horizontal disconnection of this dipping layer by the present block tectonics, so that this layer is limited to the Waiwera Block only (Fig. 1).

In the following, the five different assumptions on the hydraulic contribution of the north-south fault geothermal fluid source term and the dipping layer are introduced.

The first hypothesis tested in the present study is the inflow of geothermal fluid at a reduced temperature, i.e.

Table 2 Overview of investigated hypotheses and reference simulations in the present study

Tab. 2 Übersicht der durchgeführten Simulationen zu den untersuchten Hypothesen

Hypothesis	North-south fault section properties	Dipping layer implementation
Reference	Inflow at 50 °C	–
1	Inflow at 33 °C	–
2	No inflow	–
3	Inflow at 50 °C	Entire north-south model extent
4	Inflow at 50 °C	Limited to Waiwera Block
5	Inflow at 33 °C	Limited to Waiwera Block

33 °C instead of 50 °C, in the most-northern section of the north-south fault. This decrease in temperature may result from mixing with fluids entering the system from more shallow depths or increased residence times in the fault system, and an associated cooling, due to lower hydraulic fault conductivities in the respective fault system. Figure 3a shows the geothermal fluid source term location with an isotherm at 50 °C. The northern section of the fault (green dotted line) exhibits an inflow temperature of only 33 °C.

The second hypothesis investigated here is on the complete lack of geothermal fluid inflow in the northern section of the fault illustrated in Fig. 3 (green dotted line) as a result of the respective fault block being hydraulically inactive.

Hypothesis 3 is based on the photogrammetric mapping findings at the Waiwera beach front, suggesting the presence of a highly permeable fracture system dipping into the Waiwera reservoir. Figure 3 further illustrates the implementation of the dipping layer (light grey colour) in the simulation model, whereas the geothermal fluid source term is similarly defined as that in the reference simulation. The horizontal and vertical permeabilities of the highly permeable layer are $3.0 \cdot 10^{-11}\,\text{m}^2$ and $1.5 \cdot 10^{-11}\,\text{m}^2$ in all scenarios, respectively, while porosity is 0.12 as for the Waiwera reservoir. The parameter values were derived from the average reservoir transmissivity in the full-extent dipping layer case (Hypothesis 3) and maintained as constants in the Hypothesis 4 and 5 simulations.

A dipping layer as in the previous hypothesis, but limited to the area of the Waiwera township by block tectonics is assumed in Hypothesis 4, with geothermal fluid inflow according to the assumptions made for the reference simulation (dark grey colour in Fig. 3). Finally, Hypothesis 5 assumes geothermal fluid inflow in the northern section of the north-south fault at a temperature of 33 °C as in the Hypothesis 1 simulations, and a tectonically limited extension of the dipping layer as in Hypothesis 4.

Results and discussion

The results of the reference simulation are presented in Fig. 4a with the 38 °C isotherm and 400 mmol l⁻¹ isochlor. The geothermal fluid inflow strongly mitigates seawater intrusion into the Waiwera reservoir, whereby a wider geothermal plume is observed in the vicinity of the stronger geothermal source term located below the Waiwera township. In view of the agreement between observed and simulated temperatures plotted in Fig. 5, it becomes clear that the deviations in comparison to the profiles for boreholes B49, J.B. Schiska and V. Schiska, are significant. These findings are identical to those made by Kühn and Stöfen (2005), since the same model setup and parametrisation were applied here. Given the deviations between
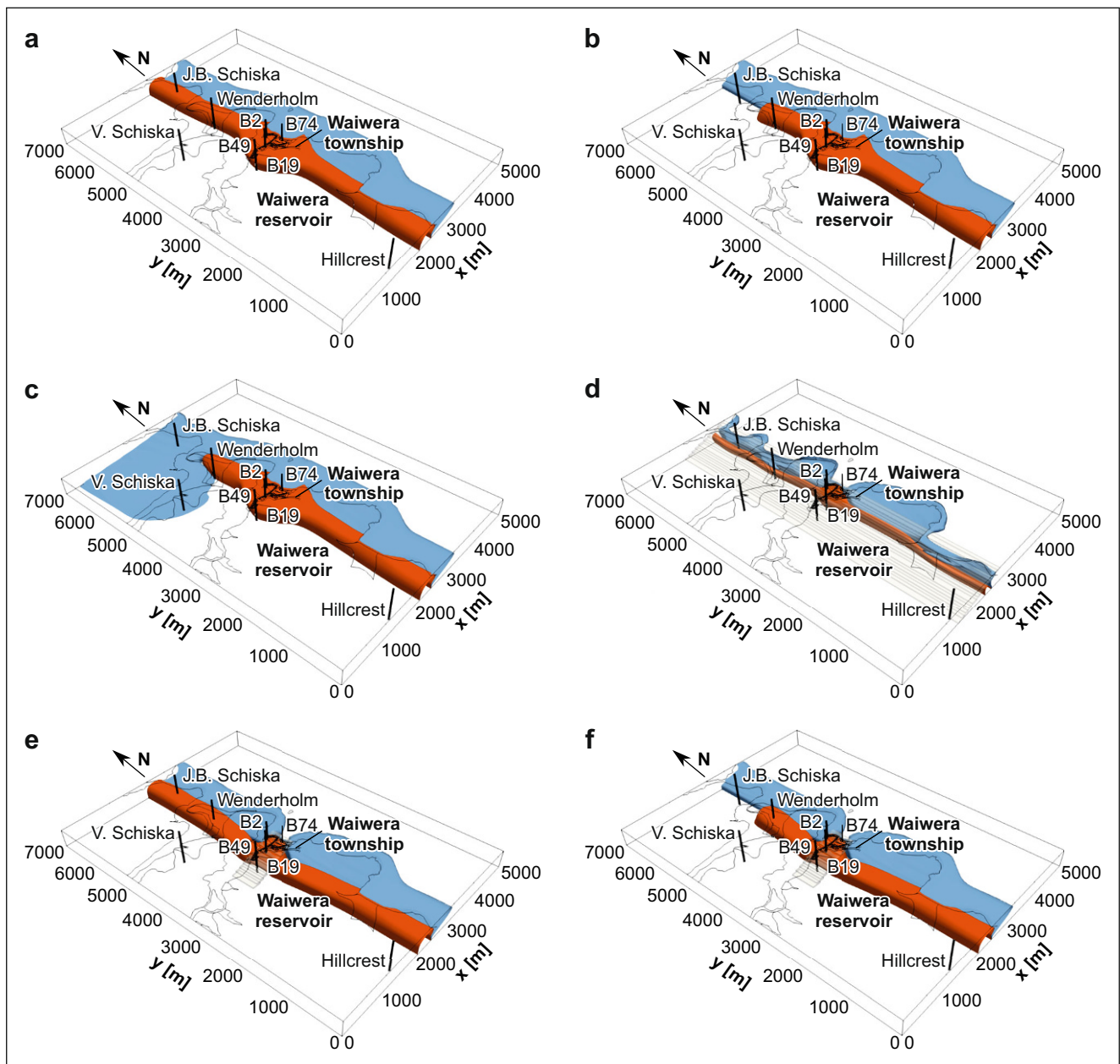
Fig. 4 Temperature and salinity distribution in the **a** reference simulation and for the Hypotheses **b** 1—limited geothermal fluid temperature in northern fault section, **c** 2—no geothermal fluid inflow in northern section of north-south fault, **d** 3—presence of highly permeable dipping layer along entire north-south extension of the model, **e** 4—presence of highly permeable dipping layer along entire north-south extension of the model limited to Waiwera township extent by block tectonics, and **f** 5—presence of highly permeable dipping layer along entire north-south extension of the model limited to Waiwera township extent by block tectonics and limited temperature of geothermal fluid in northern fault section, with 38 °C isotherm (*red*) and 400 mmol l^{-1} isochlor (*blue*) in spatial relation to the observation boreholes and Waiwera township

Abb. 4 Räumliche Verteilung der Temperatur und Salinität in der **a** Referenzsimulation und den Hypothesen **b** 1—reduzierter geothermischer Wasserzufluss im nördlichen Bereich der Nord-Süd-Störungszone, **c** 2—kein geothermischer Wasserzufluss im nördlichen Bereich der Nord-Süd-Störungszone, **d** 3—Vorhandensein einer höher durchlässigen, einfallenden Schicht entlang der gesamten Nord-Süd-Erstreckung des Modells, **e** 4—Vorhandensein einer höher durchlässigen, durch Blocktektonik begrenzten, einfallenden Schicht, und **f** 5—mit einer höher durchlässigen, durch Blocktektonik begrenzten, einfallenden Schicht mit reduziertem geothermischen Wasserzufluss. Die 38 °C-Isotherme ist durch die *rote* und die 400 mmol l^{-1}-Isochlore durch die *blaue* Isofläche im räumlichen Bezug zur Stadt Waiwera und den Beobachtungsbohrungen dargestellt
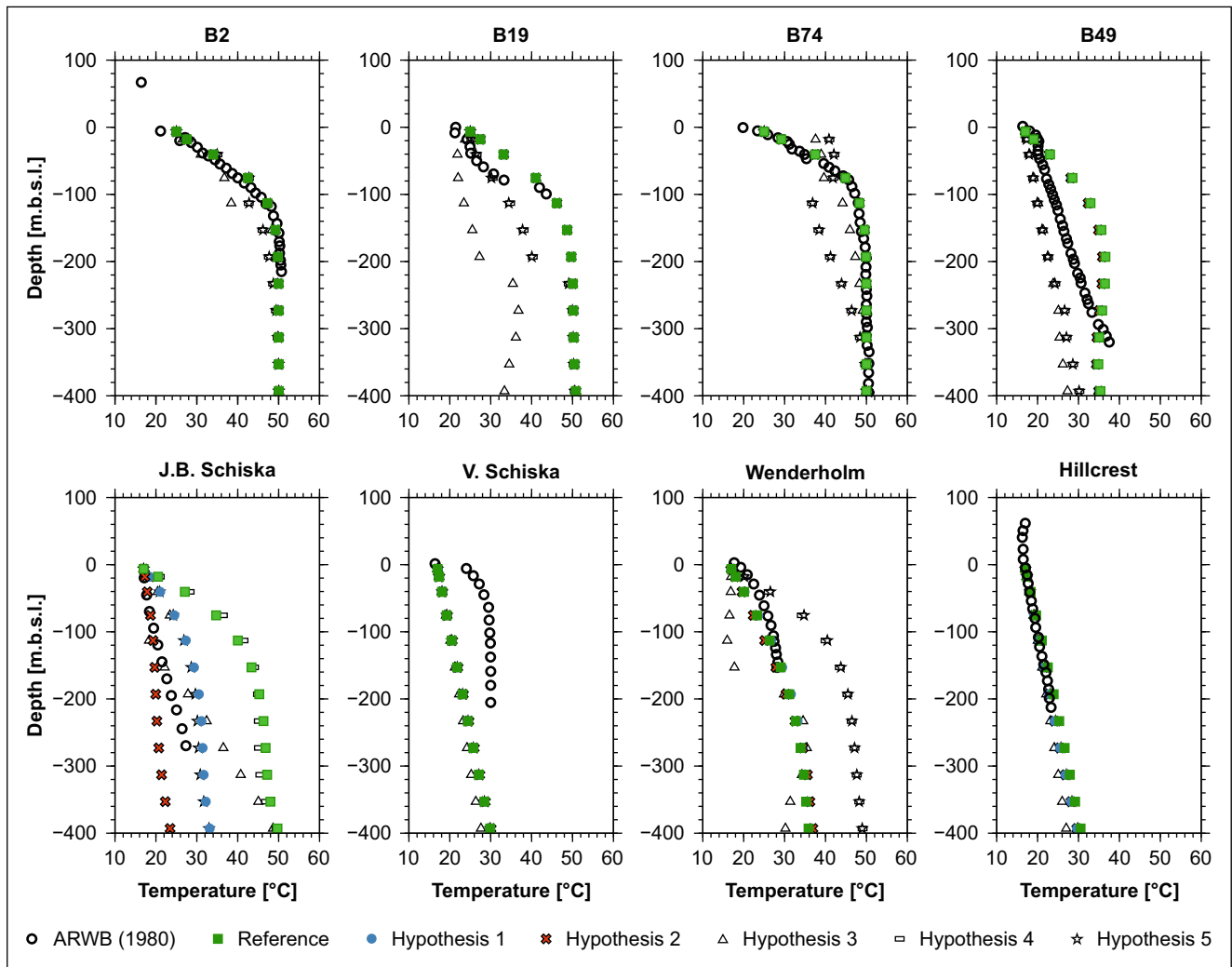
Fig. 5 Temperature profiles observed and simulated for the reference and five hypotheses cases. Near-field boreholes are plotted in the upper row, while the far-field ones are in the lower one

Abb. 5 Beobachtete und simulierte Temperaturprofile für das Referenzszenario sowie die fünf untersuchten Hypothesen. Bohrungen im Nahfeld der Stadt Waiwera sind in der oberen und jene im Fernfeld in der unteren Zeile dargestellt

observations and the reference simulation results, the hydrogeological model of the Waiwera reservoir requires further revisions to improve the overall agreement.

Figure 4b presents the results of the Hypothesis 1 simulation, whereby seawater intrusion is limited by the geothermal fluid source term in the north. However, the fluid temperature in the northern section of the north-south fault is lower. Figure 5 shows that the overall agreement with the temperature profiles is similar to that of the reference simulation, whereas the agreement with the temperature profile observed at the J.B. Schiska borehole is substantially improved. The simulated curve development proves the presence of thermal convection in the model which is notably lower than that in the reference simulation. Hence, hydraulic fault properties of the most northern section of the

north-south fault may be influenced by the tectonic block structure suggested by Alldred (1980).

Hypothesis 2 induces a seawater intrusion into the northern part of the model due to the lack of a counteracting force that was previously resulting from the geothermal fluid inflow into that area (Fig. 4c). Consequently, the geothermal fluid source seems to be the reason that it is not observed, and therefore probably not the case. All other regions exhibit identical behaviour to the reference and Hypothesis 1 simulations. As illustrated in Fig. 5, only minor deviations to the reference and Hypothesis 1 simulation results are found, except for the J.B. Schiska borehole, where the temperatures are even below those observed, demonstrating the complete lack of thermal convection and a thermal profile of the reservoir areas mainly influenced by seawater.

The spatial extent of the geothermal temperature plume is significantly reduced in the Hypothesis 3 simulation, which takes into account a highly permeable dipping layer from the Waiwera beach front into the Waitemata reservoir sandstone. This is due to the fact that the geothermal fluid is preferentially guided upwards into the seawater via the highly permeable layer. At the model top, the geothermal fluid leaves the model across the open boundary condition (Fig. 4d). Figure 5 demonstrates that the geological setting introduced in Hypothesis 3 is not likely for the Waiwera reservoir, since strong deviations from the observed temperature profiles occur for boreholes B19, B49, J.B. Schiska and Wenderholm. Consequently, block tectonics defining the presence of the layer along the extension of the north-south fault need to be considered to test if an improvement of the overall agreement between observations and simulations can be achieved based on a highly permeable dipping layer.

As a result of the findings on Hypothesis 3, the follow-up hypotheses consider limitations on the north-south extent of the dipping layer introduced by block tectonics. Here, the dipping layer extent is limited to the area below the Waiwera township, representing the size of the Waiwera Block. Simulation results (Fig. 4e) illustrate that the presence of the dipping layer below the township is capable to reduce the extent of the thermal plume in that area. However, thermal profiles shown in Fig. 5 show that slight underestimations of temperature occur in all near-field boreholes (first row), while the far-field profiles match the reference simulation as expected, since no relevant changes were introduced here.

Using the Hypothesis 4 assumptions and reducing the inflow temperature in the northern section of the north-south fault to 33 °C, as in the previously discussed Hypothesis 1 simulations, results in a similar behaviour in the near-field as in Hypothesis 4 and for the far-field as in the reference simulation (Figs. 4f, 5). The quantitative agreement with the observed temperature profiles in the boreholes becomes even worse in this case.

Considering the findings of the different hypothesis simulations, the best agreements with the observations are achieved by Hypotheses 1 (geothermal inflow temperature limited to 33 °C in the northern section of the model) and 2 (no geothermal inflow in that section), whereby simulated temperatures at the B49 borehole are too high, indicating that the thermal plume is allowed to migrate too far to the west in these models, as well as the lack of thermal convection in the V. Schiska borehole. Here, the presence of a west-east trending geological fault is probably responsible for the temperature profile which is increased above the geothermal gradient (see schematic of Wenderholm Fault in Fig. 1). Interestingly, the J.B. Schiska borehole profile is in between both hypothesis simulation results, indicating

that the geothermal inflow needs to be considered, but at a lower inflow rate.

Considering the tested hypotheses in view of an improvement between observations and simulations, it needs to be stated that the reference model already captures the reservoir processes relatively well. However, there is still room for improvements, since deviations are present at the B49 borehole, where the simulated temperature exceeds the observed data, implying the presence of thermal convection at the borehole location. Further, the J.B. Schiska borehole also exhibits substantially increased temperatures according to the simulations, indicating the presence of a much stronger geothermal source at the reservoir bottom, while an almost linear geothermal gradient with half the temperature is observed. Furthermore, the simulations do not show the geothermal convection impact observed in the V. Schiska borehole.

The tested hypotheses (Hypotheses 1 and 2) on a potentially limited impact of the most-northern section of the north-south fault in terms of lower geothermal fluid temperatures and a complete absence of fluid inflow in that section show that the hydraulic impacts resulting from the tectonic block structure of the reservoir are likely responsible for the reference model's deviation in the J.B. Schiska borehole. Interestingly, the observed temperature profile lies well in between the reduced temperature (Hypothesis 1) and no-inflow assumptions (Hypothesis 2). This demonstrates that this fault section cannot be decoupled from the hydraulically active north-south fault system, as fluid inflow is required to not underestimate the thermal impact. Nevertheless, the almost linear profile of the observed temperature in that borehole suggests only a minor impact of thermal convection, starting at about 150 m depth.

The initial main motivation of the present study, namely testing the influence of the recently discovered dipping layer on the thermal profiles observed in the boreholes, has revealed a significant impact on the overall simulated temperatures. However, all investigated scenarios induce an increase in the deviations between the simulated and observed temperature profiles (Hypotheses 3, 4 and 5), whereby all near-field boreholes show simulated fluid temperatures which are too low. On the other hand, temperatures are above or below those observed in the far-field boreholes J.B. Schiska, V. Schiska and Wenderholm. Nevertheless, almost all investigated hypotheses do not significantly alter the agreement for the Hillcrest borehole, except for a slight underestimation starting below 250 m depth by the Hypothesis 3 simulations (dipping layer with full north-south extent).

Borehole B49 is not matched well by any of the simulations, indicating that a structural geological feature may be responsible for the observed temperature profile. Here, the simulations without the dipping layer overestimate the

contribution of thermal convection, while the introduction of the dipping layer underestimates the temperature observations. Moreover, the latter simulations exhibit an almost linear temperature profile following the geothermal gradient. Contrary to the J.B. Schiska borehole, a structural geologic feature such as the dipping layer is likely required here to deviate the geothermal fluid flow away from the B49 borehole. The temperature profile at the V. Schiska borehole is not matched by any of the simulations. Here, the authors assume the presence of a yet not documented west-east trending fault which may be dividing the Wenderholm Block, since a clear signal of a geothermal convection, i.e. disturbance of the natural geothermal gradient is observed.

Summary and conclusions

Recently acquired field data proves the presence of a previously unverified fault, trending in the north-south direction along the Waiwera beach front. Further, photogrammetric mapping shows that hot fluids enter the sea via fracture systems, likely connected to the Waiwera geothermal reservoir (Präg 2020; Präg et al. 2020). Considering these new findings, the objective of the present study was to test and revise the reference reservoir model previously introduced by Kühn and Stöfen (2005), so that it becomes applicable for sustainable water management. In this regard, five hypotheses were tested to account for the documented tectonic block structure (Alldred 1980) of the reservoir as well as the presence of a highly permeable layer dipping into the reservoir from the beach front. All simulation results were compared against the observed data and it was verified that the reference model is indeed improved by introduction of the geological findings of the recent field campaigns.

Although new insights were obtained and substantial progress was made in view of understanding and verifying the impacts of the north-south fault hydrogeology, including the presence of a highly permeable layer dipping into the Waiwera reservoir, further model revisions are required to improve the results at the B49 and V. Schiska boreholes. These tasks will be supported by additional field campaigns including geophysical methods such as 2D seismics as well as geophysical and hydrogeological borehole measurements, supported by remote sensing in the next step to increase the data base on borehole temperatures, coastal seawater intrusion and potential fracture networks as well as the currently known and unknown geologic faults. These data will support simulation model refinements to provide reliable predictions for the further development of the regional water management plan.

References

Alldred, H.B.: Sedimentology and structure of the Waitemata Group Wenderholm & Orewa Section (1980)

Alvarez, J.: A reservoir model of the Waiwera warm water system. Report No. 86.02, Geothermal Institute, University of Auckland., p. 32 (1986)

Auckland Regional Water Board: Waiwera water resource survey: preliminary water allocation/management plan. Technical Publication, Issue 17. Auckland Regional Water Board, Auckland, p. 178 (1980)

Auckland Regional Water Board: Waiwera thermal groundwater: allocation and management plan Technical Publication, No. 39. Auckland Regional Water Board, Auckland, p. 151 (1987)

Bell, I.H., Wronski, J., Quoilin, S., Lemort, V.: Pure and pseudo-pure fluid thermophysical property evaluation and the open-source thermophysical property library coolprop. Ind. Eng. Chem. Res. **53**, 2498–2508 (2014). https://doi.org/10.1021/ie4033999

Bréthaut, D.: Numerical modelling of the Waiwera geothermal system. Project report—GEOTHERM 689. The University of Auckland, Auckland, p. 37 (2009)

Chabab, E., Kühn, M., Kempka, T.: Upwelling mechanisms of deep saline waters via Quaternary erosion windows considering varying hydrogeological boundary conditions. Adv. Geosci. **58**, 47–54 (2022). https://doi.org/10.5194/adgeo-58-47-2022

Chapman, M.G.: Investigation of the dynamics of the Waiwera geothermal groundwater system, New Zealand. Master Thesis, 56 p, The University of Waikato, Hamilton, New Zealand (1998)

Driesner, T., Heinrich, C.A.: The System H2O-NaCl. I. Correlations for molar volume, enthalpy, and isobaric heat capacity from 0 to 1000 degrees C, 1 to 5000 bar, and 0 to 1 X-NaCl. Geochim. Cosmochim. Acta **71**, 4902–4919 (2007)

Kempka, T.: Verification of a Python-based TRANsport Simulation Environment for density-driven fluid flow and coupled transport of heat and chemical species. Adv. Geosci. **54**, 67–77 (2020). https://doi.org/10.5194/adgeo-54-67-2020

Kempka, T., Steding, S., Kühn, M.: Verification of TRANSPORT Simulation Environment coupling with PHREEQC for reactive transport modelling. Adv. Geosci. **58**, 19–29 (2022). https://doi.org/10.5194/adgeo-58-19-2022

Kühn, M., Altmannsberger, C.: Assessment of data driven and process based water management tools for the geothermal reservoir Waiwera (New Zealand). Energy Procedia **97**, 403–410 (2016). https://doi.org/10.1016/j.egypro.2016.10.034

Kühn, M., Grabow, L.: Deconvolution well test analysis applied to a long-term data set of the Waiwera geothermal reservoir (New Zealand). Adv. Geosci. **56**, 107–116 (2021). https://doi.org/10.5194/adgeo-56-107-2021

Kühn, M., Schöne, T.: Multivariate regression model from water level and production rate time series for the geothermal reservoir Waiw-

era (New Zealand). Energy Procedia **125**, 571–579 (2017). https://doi.org/10.1016/j.egypro.2017.08.196

Kühn, M., Schöne, T.: Investigation of the influence of earthquakes on the water level in the geothermal reservoir of Waiwera (New Zealand). Adv. Geosci. **45**, 235–241 (2018). https://doi.org/10.5194/adgeo-45-235-2018

Kühn, M., Stöfen, H.: A reactive flow model of the geothermal reservoir Waiwera, New Zealand. Hydrogeol J **13**(4), 606–626 (2005). https://doi.org/10.1007/s10040-004-0377-6

Kühn, M., Altmannsberger, C., Hens, C.: Waiweras Warmwasserreservoir – Welche Aussagekraft haben Modelle? Grundwasser **21**(2), 107–117 (2016). https://doi.org/10.1007/s00767-016-0323-2

Kühn, M., Präg, M., Becker, I., Hilgers, Ch , Grafe, A., Kempka, T.: Geographic Information System (GIS) as a basis for the next generation of hydrogeological models to manage the geothermal area Waiwera (New Zealand). Adv. Geosci. **58**, 31–39 (2022). https://doi.org/10.5194/adgeo-58-31-2022

Lam, S.K., Pitrou, A., Seibert, S.: Numba: a LLVM-based python JIT compiler. In: Proceedings of the second workshop on the LLVM compiler infrastructure in HPC, LLVM '15. Association for Computing Machinery, New York (2015) https://doi.org/10.1145/2833157.2833162

Li, Z., Spangenberg, E., Schicks, J.M., Kempka, T.: Numerical simulation of hydrate formation in the LArge-scale reservoir simulator (LARS). Energies **15**, 1974 (2022a). https://doi.org/10.3390/en15061974

Li, Z., Spangenberg, E., Schicks, J.M., Kempka, T.: Numerical simulation of coastal sub-permafrost gas hydrate formation in the Mackenzie Delta, Canadian arctic. Energies **15**, 4986 (2022b). https://doi.org/10.3390/en15144986

OpenMP: OpenMP architecture review board. Application program interface version 3.0. May 2008 (2008). https://www.openmp.org/mp-documents/spec30.pdf. Accessed 29_June 2023

Otto, C., Steding, S., Tranter, M., Gorka, T., Hámor-Vidó, M., Basa, W., Kapusta, K., Kalmár, I., Kempka, T.: Probability of contaminant migration from abandoned in-situ coal conversion reactors. Adv. Geosci. **58**, 55–66 (2022). https://doi.org/10.5194/adgeo-58-55-2022

Parkhurst, D.L., Appelo, C.A.J.: Description of input and examples for PHREEQC version 3—A computer program for speciation, batch-reaction, one-dimensional transport, and inverse geochemical calculations (2013). https://pubs.usgs.gov/tm/06/a43. Accessed 29_June 2023

Präg, M.: Geothermal reservoir characterization of faulted and folded turbidite sequences, Waiwera, New Zealand. MSc thesis, Karlsruhe Institute of Technology—KIT, 86 p (2020, unpublished).

Präg, M., Becker, I., Hilgers, C., Walter, T.R., Kühn, M.: Thermal UAS survey of reactivated hot spring activity in Waiwera, New Zealand. Adv. Geosci. **54**, 165–171 (2020). https://doi.org/10.5194/adgeo-54-165-2020

Pruess, K., Schroeder, R.C.: Geothermal reservoir simulations with SHAFT-79. Lawrence Berkley National Laboratory, Berkley, p. 10 (1979)

Pruess, K., Oldenburg, C., Moridis, G.: TOUGH2 userís guide. Version 2.0. Lawrence Berkeley Laboratory Report LBL-43134. Lawrence Berkley National Laboratory, Berkeley (1999)

Schofield, J.C.: Geological Map of New Zealand—Helensville and Whangaparaoa (1989)

Sharqawy, M.H., Lienhard V, J.H., Zubair, S.M.: Thermophysical properties of seawater: A review of existing correlations and data, Desalin. Water Treat. **16**(1–3), 354–380 (2010). https://doi.org/10.5004/dwt.2010.1079

Somogyvári, M., Kühn, M., Reich, S.: Reservoir-scale transdimensional fracture network inversion. Adv. Geosci. **49**, 207–214 (2019). https://doi.org/10.5194/adgeo-49-207-2019

Steding, S., Kempka, T., Kühn, M.: How insoluble inclusions and intersecting layers affect the leaching process within potash seams. Appl. Sci. **11**, 9314 (2021a). https://doi.org/10.3390/app11199314

Steding, S., Kempka, T., Zirkler, A., Kühn, M.: Spatial and temporal evolution of leaching zones within potash seams reproduced by reactive transport simulations. Water **13**, 168 (2021b). https://doi.org/10.3390/w13020168

Urquhart, A., Bauer, S.: Experimental determination of single-crystal halite thermal conductivity, diffusivity and specific heat from –75 °C to 300 °C. Int. J. Rock Mech. Min. Sci. **78**, 350–352 (2015). https://doi.org/10.1016/j.ijrmms.2015.04.007

Van Rossum, G., Drake, F.L.: Python 3 reference manual. CreateSpace, Scotts Valley (2009)

Von Schroeter, T., Hollaender, F., Gringarten, A.C.: Deconvolution of well test data as a nonlinear Total Least Squares problem. Spe J. (2013). https://doi.org/10.2118/71574-MS

Zermansky, G.: Hydrogeological evaluation of the Waiwera geothermal aquifer. Client report 2005/131. GNS Institute of Geological & Nuclear Science, Wellington, 56 p (2005).